Journal of Solar Energy Research (JSER)

Journal homepage: www.jser.ut.ac.ir

Integrated Assessment of Energy Storage and Thermal Losses in a Paraffin-Enhanced Solar Air Heater for Efficient Room Heating

Salah H. Abid Aun*, Afaq Jasim Mahmood, Hussein M. Al-Mrayatee

Middle Technical University, Polytechnic College of Engineering Specializations, Baghdad, Iraq

ARTICLE INFO

Article Type:

Research Article

Received:2025.11.22
Accepted in revised form:2026.01.01

Keywords:
PCM;
Collector;
Intensity;
Convection;
Radiation

A B S T R A C T

This paper presents an experimental investigation of the thermal performance, energy-storage capability, environmental impact, and financial feasibility of a dual solar air heater using paraffin wax as a phase change material (PCM) and a perforated absorber plate. The system was tested under actual winter weather conditions at airflow rates ranging from minimum 0.017 kg/s to maximum 0.032 kg/s to evaluate the useful thermal energy gain, heat loss, outlet air temperature, and overall thermal efficiency. The results show that at the optimal airflow rate 0.026 - 0.032 kg/s, the system produced approximately 32.36 MJ/day of net useful thermal energy—sufficient to raise the temperature of an indoor space of 2,677 m³ by 10 °C. A maximum thermal efficiency of 78% was achieved with a relatively low total heat loss of 205 W. In contrast, the maximum outlet temperature of 64 °C occurred at the lower airflow rate of 0.017 kg/s, which resulted in higher heat losses due to convection and radiative of 296 W. These increased losses caused a 10% reduction in thermal efficiency. Based on Iraq's national thermal-energy emission factor of 0.95 kg CO_2 /kWh, the system has the potential to reduce annual carbon dioxide emissions by approximately 1.86 metric tons.

1. Introduction

Long-term energy storage systems based on phase change material (PCM), in particular, paraffin wax have aroused much promise when it comes to system use beyond the laboratory. They are ideal to be utilized with a high variety of energy-saving technologies out there, as they work passively, they are modular, and they are able to store a significant amount of latent heat. PCM may be applied to dry crops in agriculture, maintain temperature in the textile and paper sectors, and warm areas by installing thermal storage units in the building walls, ceilings, or floors to store solar heat during the day and

*Corresponding Author Email: dr.salah_haji102@mtu.edu.iq

Cite this article: Abid Aun, S. Haji, Mahmood, A. Jasim and Al-Mrayatee, H. Mohammed (2025). Integrated Assessment of Energy Storage and Thermal Losses in a Paraffin-Enhanced Solar Air Heater for Efficient Room Heating. Journal of Solar Energy Research, 10(4), 2672-2690. doi: 10.22059/jser.2026.406779.1671

DOI: 10.22059/jser.2026.406779.1671

generate it during the night [1-3]. The collector itself is stuff and this is the key component of a solar collector that converts sunlight to an essential thermal energy. The target of continued research is to ensure that the system becomes more flexible and works. The most common material that has been used in storing thermal energy over a long period is paraffin wax due to the presence of the right melting point, it is chemically stable, it is readily available and it is also very economical [4]. Qusay et al. [5] improved the thermal conductivity of paraffin by adding paraffin nanoscale silicon carbide (SiC) particles. This addition also heightened the viscosity as well as the density hence boosting the outlet temperatures. The peak temperature of 64.4 oC was attained between 1 and 3 p.m. The system stored the heat as well over three hours beyond the sunset. Abdulmunem et al. [6] included paraffin wax longitudinal fins to enhance absorption of heat. This modification was an improvement on a collector in which only paraffin was placed in the thermal storage to make the collector effective. They have also assessed the loss of heat in various test conditions to observe the influence of the loss of heat on collectors. The paraffin wax and fins collector took approximately 24 and 33 percent of the energy of the collector that had no fins during the maximum charging time (12:30 p.m.).

For Singh et al. [7], the thermal performance was evaluated on a face of a plate absorber and a serrated geometry of an absorber, to study the behavior with and without the use of a phase change material (PCM). The findings indicated that even at 21 ^{o}C the efficiency of a serrated-plate solar air heater (SAH) with PCM remained approximately 19 percent higher than the efficiency of a non-PCM SAH. In the absence of PCM it was approximately 23 higher. In a bid to increase heat transfer rate between the absorber surface and the phase change material, researchers Mahto et al. [8] explored the use of paraffin wax immersed pin-fin absorber plate. This altered the thermal conductivity of the emitted air as well as improving thermal energy storage. PCM was applied on either side of the solar air heater in another set-up and 8 ribs were included. It was found that the eight-ribbed PCM twin solar air heater was better than other designs in terms of thermal performance. The applicability of PCM made the air exiting the outlet a lot hotter and the heat release was up to two hours following the setting of the sun [9].

Past analyses have demonstrated that the rate of melting of the paraffin can be reduced in terms of rate by augmenting the airflow rate and decreasing the melting point in the change of phase. It is also stated that the temperature and thermal efficiency of a solar air heater depends on the quantity of air being passed through it as well as the quantity of sunlight. The maximum temperature rise of 17.95 ^{o}C above average airflow rate of 0.01 kilogram per second was experienced and at the same time 825 W/m^2 maximum solar intensity was recorded [10].

Fath [11] examined the actions of a conventional solar air heater (SAH); the investigators used paraffin wax, which is a phase change material (PCM), the melting point of which is 50 ^{o}C. The method involved capsules of wax in copper cylindrical form corrugated and subsisted as absorbers and storage of heat. The collector had a surface area of 1.0 m^2 and a gap of air of 0.075 m. It was demonstrated by experimental findings that the daily performance of the PCM capsules in a staggered configuration was about 63.35% at a rate of 0.02 kg/s. This configuration had the outlet air temperature of approximately 5 ^{o}C above ambient and held constant during almost 16 hours, and a flat plate SAH with only 38.7 percent daily efficiency over 9 hours. In the same way, the Charvat et al. [12] studied a solar air heater installed with the encapsulated PCM modules in the air duct to enhance the heat storage capacity. Their findings affirmed that with the addition of PCM the thermal stability of the outlet air temperature was greatly increased and the system had a longer working life as compared to traditional designs with no thermal storage. According to the research undertaken by Researchers Agyenim et al. [13], the PCM storage was comprised out of 3 mm thick horizontally mounted cylindrical aluminum shell with an inner diameter of 146.4 mm.

The control set-up (single tube system) was to use a copper tube that was embedded into the PCM and served as the heat transfer tube with a diameter of 54 mm. The second was the multi-tube-type (shell same dimensions, but with 4 cylindrical heat transfer tubes with a diameter of 28 mm spacing 120 mm). The multi-tube system was shown to be much more efficient in the rate of heat transfer during the charging process, gave higher results in outlet temperatures, and proved very practical when using PCM as a thermal energy source especially because of its sizeable capacity of storing heat.

The researchers Tyagi et al. [14] investigated the case of nanoparticles being incorporated into paraffin wax in order to improve its thermal conductivity. Considering the severe drawbacks of the use of paraffin, the use of other strategies, including the inclusion of nanoparticles or Nano capsulation methods has produced encouraging results in terms of

enhancing heat uptake and lowering the thermal losses.

Moreover, the authors Shalaby et al. [15] investigated the inclusion of expanded graphite, carbon fibers, and good thermal conductor materials like graphite foam on paraffin wax and results have shown that the thermal conductivity of the solar systems has been made significantly better. It has also been noted in many studies that perforated baffle plates are used to improve the performance of solar air heaters. The holes enable the air to enter through the specific holes, derailing the laminar flow and causing turbulence. Such a change of laminar to turbulent flow enhances the heat transfer coefficient that makes solar energy transfer in the flowing stream of air more efficient [16]. Capsules that were used in the design mentioned in [17] were paraffin wax filled and eight galvanized iron pipes. The results indicated that the higher the airflow rate at 0.03 kg/s the lower the PCM melting temperature and the longer the period it took to melt. Thus, the practical energy productivity had risen up to 160 W, and the efficiency of thermal storage had been amplified. Perforated plates installed in heat exchangers are not a novel concept as the initial installations were made in 1949 and installed across the direction of the airflow [18].

Numerous investigations have followed since that time of the role of turbulence promoters and the devices troubling the flow in solar air heater. Circular or square holes, triangular pitch layout arrangements have among other things been demonstrated to enhance the coefficient of the airside heat transfer considerably due to their ability to distort the boundary layer and generate turbulent flow [19]. Experimental and numerical researches have demonstrated positive findings especially in ducts with rectangular configurations and are fitted with circular perforations and square holes' ducts fitted by ribs or perforated ribs of different configurations. Such changes have shown significant enhancement on thermal energy capture and this feature enhances more effective performance of solar collector [20]. A study conducted by Sara et al. [21] examined the effectiveness of a rectangular solar air heater by placing four sided, holes on the absorber surface of a collector using block-shaped plates that had four sides. Their findings showed that perforated block structure was superior to the transverse blocks that were not perforated. Although solid barriers are easier to allow heat in, the strength of increase in the friction factor that it introduces is still a formidable issue [22]. The perforative barriers allow some of the air to pass through the holes and this reduces bad effects such as increase in the drag and overheating in some areas. This design assists in ensuring that air flows in the duct with less difficulty, and it prevents the occurrence of hot spots [23]. Similar study was done by Arunkumar et al. [24], who studied the effectiveness of a solar air heater duct, in which the perforated part was in two-row format with 5 mm diameter openings. According to their findings, there was a significant increase in their thermal efficiency to an optimum of 83.01 percent in the best conditions.

This research aims at enhancing the efficiency and lifespan of a flat-plate solar air heater using the combination of a perforated plate of absorber and paraffin wax. The available literature suggests that no research has been conducted hitherto incorporating the use of the perforated plate of absorber with the inclusion of a phase change material (PCM). This experiment enhanced the capacity of the solar collector to absorb heat through placing paraffin wax under a perforated semitransparent absorber driven by a 105 × 100 cm2 perforated absorber plate. The holes that are perforated in the plate allow air to flow faster through them thus increasing the heat transfer coefficient. Paraffin wax on the other hand is a good method of retaining latent heat. The airflow rate of 0.026 and 0.032 kg/s resulted in the system losing less heat and absorbing more energy. This was a two-solar collector design that optimized the performance of the heater to retain the heat. To establish whether it was working, the lab had a 210 m2 area that was then heated. The air that exited the two collectors was hotter when the paraffin wax was included. The research considered the functionality of the system in the actual situation of Iraq and the way it can benefit the environment reducing the emission of CO_2.

2. Experimental Arrangement/ Methodology and Experimental Setup

This study experimentally investigates the energy-storage behavior, thermal performance and overall efficiency of a dual solar air heater take in a perforated absorber plate and paraffin wax as a phase change material (PCM). All measurements were conducted under real winter weather conditions. The solar air heater consists of a transparent glass cover, a perforated absorber plate, and a set of paraffin-wax tubes positioned above the absorber. The entire unit is enclosed within a well-insulated wooden frame. Airflow was supplied by a fan, with mass flow rates controlled between 0.017 and 0.032 kilogram per second. Type-K thermocouples were installed at the air inlet, outlet, PCM sections, and in the ambient environment to record temperature variations. Incident solar radiation was measured using a

pyranometer. Measurements collected during the experiment included: Solar radiation (W/m²), Inlet (Ti), outlet (To), and ambient air temperatures (Ta), PCM temperature, Airflow rate (kg/s), Heat losses (W) and useful thermal gain (W) calculated from measured data. Temperature readings and solar

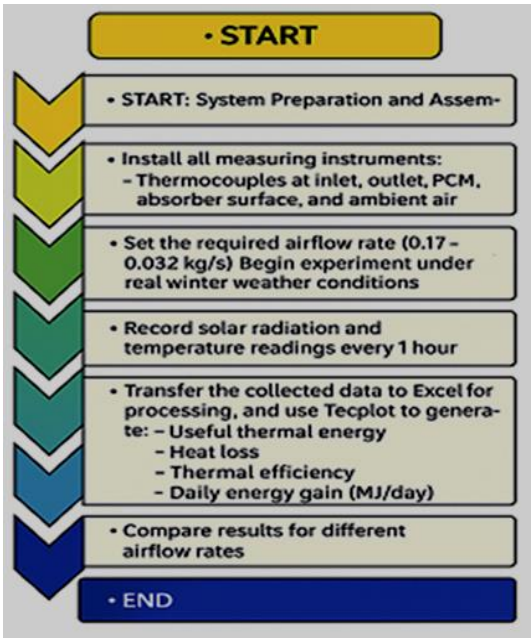

radiation values were taken at every one hour

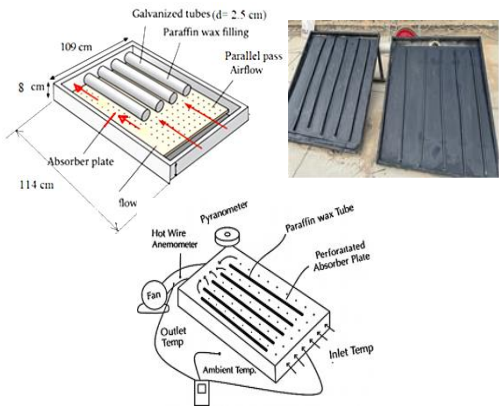

intervals throughout the day.

(a)

(b)

Figure 1. (a) Flowchart of the Experimental Procedure, (b) Scheme and photos of the experimental work

All recorded measurements were processed using Microsoft Excel. The software was used to organize raw temperature and radiation datasets and compute useful thermal energy, heat loss, and thermal efficiency. To analyze and visualize the experimental data, temperature trends, solar-radiation profiles, and energy-performance curves were plotted using Tecplot software. Small plastic straw tubes measuring 5 mm in diameter and 40 mm in length were positioned 110 mm downstream of the outlet to ensure a more uniform distribution of the airflow. Heat losses through the insulated surfaces were considered negligible, as the entire body of the heater was thoroughly insulated. Below is a Flowchart of the Experimental Procedure as a Figure (1a).

2.1 Test Facility Description

This study encompasses the design and construction of two flat-plate solar air heaters intended for the preheating of the mechanical engineering workshop at the (33.33°N, 44.43°E) Middle Technical University– Polytechnic College of Engineering Specializations, Baghdad. The solar air heater units were made of wood and were set up so that they faced south at a 41° angle to get the most sun exposure for more than nine hours a day. The primary performance-enhancing components of the system are the absorber plate and the transparent cover, both of which are designed to increase heat-transfer rates and improve airflow dynamics. All the collectors have rectangular perforated plate of galvanized steel with a thickness of 1.5 mm with ten paraffin wax tubes (2.5 cm in diameter and 100 cm in length). Photo reactive area of the glass cover (6 mm thick) and the absorber plate is 114 × 105 mm^2, it functions to absorb solar radiation, reduce thermal losses to the environment, increase the outlet air temperature, and ultimately enhance the overall effectiveness of the system. To further improve solar absorption, all internal surfaces of the solar canal, including the holed plate and paraffin wax tubes, were painted black. The design aims to utilize both convective heat transfer enhancement through the holed plate and thermal storage via the embedded phase change material (PCM). Figure 1b presents a photographic and scheme of the experimental test bed. The collector structure features a rectangular wooden duct with a test space depth of 0.08 m and a surface area of 1.14 × 1.09 m^2. The detailed specification of the collector in addition the measurement equipment used in this study are listed in Table 1.

Table 1. Specifications and Details for Solar Collectors and Measurement Equipment

performance	Description
Location of dual solar collectors	(Longitude: 44.43°E Latitude:33.33°N,) city of Baghdad
Collector material and Sizes efficiency	Dualwooden collectors, each measuring 1.14m× 1.09 m × 0.08 m
Orientation & Tilt Angle	South-facing, inclined at 41°.
Cover Materials	Glass panel (surface area: 114 cm × 105 cm).
Inlet Opening Area	Rectangular opening: 8 cm × 114 cm
Outlet Opening	Circular outlet diameter: 8 cm
Perforated Plate	Hole diameter: 0.21 cm; hole spacing (pitch): 4 cm; mounted parallel to base
Pyrometer	Model: 200-03 RK, Max. Range: 2000 W/m², Serial No.: R18021068
Centrifugal Fan	Model: 16A 135C, Power: 0.75 kW
Hot Wire Anemometer	Model: 9829- HT, Current: 60–90 mA
Temperature Sensor	EXTECH 200 SDL, Accuracy: (±0.5 °C) (±0.4%), using data logging capability

The perforated galvanized sheet as an absorber plate are installed parallel to the collector base, featuring holes with a diameter of 0.21 cm and spaced at a pitch of 4 cm. As air flows through these perforations, its velocity increases, which in turn enhances convective heat transfer within the collector system [26], [27]. The inlet air enters the collector through a rectangular opening measuring 8 cm × 114 cm, and exits through a circular outlet with a diameter of 8 cm.

A Hot Wire Anemometer is calibrated {model of 9829- HT, (60-90) mA}, then stationary at the deliver airflow section for determining airflow velocity. An EXTECH instrument is used for showing temperatures data. Four-channels thermometer, SDL200 model, ± (0.4 % + 0.5°C), four thermocouples is calibrated and fixed at four positions (T-type), used for the registered air temperatures, such as: Ta, ambient temperature, thermocouple fixed under the rig, Ti inlet air temperature, thermocouple stable at the middle of the air entrance to grove area of 114*4 cm^2 while, outlet temperature used two thermocouples placed in the center of the outlet airflow channel diameter of 8 cm. A pyrometer is used for measuring solar intensity in watts per square meter. The solar intensity data registration period was from the morning from eight clock to five clock at evening. The solar heat flux measured by Pyranometer which was located on glass cover of the solar platform. The solar system is designed as an active system, so the fan was placed at the back side of the collector. An inverter (from 0.01 to 400 Hz, Five Am, SV008iC5-1,) is utilized to manage a power input then adjust the fan speed, enabling control of the airflow at four different rates between 0.017 and 0.032 kg/s. The Table 1 provides a summary of the design and operating parameters.

3. Analysis of the Thermal Output

3.1 Thermal Efficiency and Heat Transfer in a Solar Collector

The amount of useful heat transferred by air through the solar collector can be estimated on the basis of the average temperature of plate absorber. This is usually checked by the use of Hottel-Whillier-Bliss equation that offers a sound system of computing thermal energy moved to the flowing air inside the solar duct. The equation takes into consideration the input of solar radiation, heat loss, system geometry, and can provide a feasible approach to the analysis of the thermal performance of the collector [28-29].

$$Q_u = A_p F_R [I(\tau\alpha) - U_L(T_i - T_a)] \quad (1)$$

Thermal efficiency ηth and heat removal factor FR of the solar collector can be determined using the following relations, which account for the collector's

ability to transfer absorbed solar energy to the working fluid under real operating conditions [25]:

$$\eta_{th} = \frac{Q_u}{I.A_p} = F_R\left[(\tau\alpha) - U_L\left(\frac{T_{i-}\ T_a}{I}\right)\right] \quad (2)$$

Alternatively, Equation (2) for useful heat gain can also is express in term of the air outlet temperature as follows [25]:

$$\eta_{th} = F_o\left[(\tau\alpha) - U_L\left(\frac{T_o - T_i}{I}\right)\right] \quad (3)$$

Where Fo is the factor that can be evaluated using the following relation, which represents the ratio of the actual useful heat gain to the maximum possible heat gain if the entire absorber were at the inlet fluid temperature [26]:

$$F_{o=}\frac{\dot{m}\,C_p}{U_L\,A_p}\left[exp\left(\frac{U_L A_p\,F'}{\dot{m}\,C_p}\right) - 1\right] \quad (4)$$

The thermal efficiency is calculated as Useful energy gain is evaluated with heat flux from sun as [29]:

$$\eta_{th} = \frac{Q_u}{I\,A_p}\ where\ Q_u = \dot{m}C_p(T_o - T_i) \quad (5)$$

3.2 Uncertainty analysis for Paraffin Collectors

The uncertainty in solar thermal efficiency (ωηth) is estimated using Holman's method, which accounts for the possible errors arising from daily experimental measurements [25–27]. Accordingly, the overall uncertainty is calculated based on the following expression, as given in Equation (6a):

$$\frac{\omega\eta}{\eta} = \left[\left(\frac{\omega\,\dot{m}}{\dot{m}}\right)^2 + \left(\frac{\omega\,\Delta T}{\Delta T}\right)^2 + \left(\frac{\omega\,I}{I}\right)^2\right]^{\frac{1}{2}} \quad (6a)$$

$$\frac{\omega\dot{m}}{\dot{m}} = \left[\left(\frac{\omega\,v}{v}\right)^2 + \left(\frac{\omega\,a}{a}\right)^2 + \left(\frac{\omega\,\rho}{\rho}\right)^2\right]^{\frac{1}{2}} \quad (6b)$$

For the paraffin-based solar collectors, the average values of (Ti) inlet temperature, (To) outlet temperature, (ΔT) temperature difference, (I) solar intensity, and (η) thermal efficiency were calculated individually for each of the four experimental days, as shown in Table 2. These daily measurements were then combined, and the overall mean values were used to evaluate the fractional uncertainty in the system's thermal performance [30]. The uncertainty in thermal efficiency was determined based on the propagation of errors associated with key influencing parameters, including the mass flow rate of air, temperature difference, solar intensity, and collector area. The combined effect of these uncertainties was used to quantify the total uncertainty in thermal efficiency for the paraffin collector configuration. The air flow rate fractional uncertainties were determined based on average data for four days of measurements. The uncertainty of the mass-flow-rate calculation using Holman's root-sum-square method (see Eq. 6b) [25-27]. where the uncertainties in velocity (ωv), duct area (ωa), and density (ωρ) were ±2 %, ±0.5 %, and ±0.5 %, respectively.

Table 2. Total average values and fractional uncertainties based on four days of experimental measurements

Variable (Average)	m	Ti	To	**Δ**T	I	η
	0.024	19.4	42.2	22.8	659.65	0.64
Uncertainty %	ω ṁ	ω Ti	ω To	ω ΔT	ω I	ω η
	±0.5	±0.5	±0.5	±0.70	±7	±2,04

4. Results and discussion

Two types of solar air heaters were experimentally investigated under identical environmental conditions and working days, as illustrated in Figure 1. Measurements of inlet and outlet air temperatures, along with solar radiation intensity, were recorded during outdoor operation over a continuous nine-hour period, from 8:00 AM to 5:00 PM. Data was manually collected at one-hour intervals throughout the day. The performance analysis was done to conclude on the quantity of useful thermal energy and thermal efficiency acquired by dual collectors. Any tests conducted were carried out at times when the weather was clear and there was no much wind disturbance so that the solar input could be very similar. The experiment was performed during four days March 16, 17, 18, and 19, 2025 and with four airflow rates of 0.017 to 0.032 kg/s occurring. The rates of airflow are consistent with the rates proposed in the scientific literature on the solar heating systems in general. All calculations were made by assuming (1007 J/kg·K) the specific heat of air at constant pressure and air

density for air temperatures around 18–22°C, (1.22 kg/m^3).

4.1 Solar Radiation with Inlet/Outlet Temperature Behavior

In this section, the variation of three key parameters during the day, which were solar radiation intensity, inlet air and outlet air, were varied by varying airflow rates. These aspects are significant to determine the effectiveness of the solar air heater and its sensitivity to the heat.

The daily solar radiation, inlet air temperature, and outlet air temperature are recorded during March 2025 to evaluate the influence of solar intensity and inlet conditions on the outlet temperature at various airflow rates. A series of curves illustrating solar radiation intensity, inlet temperature, and outlet temperature were obtained over a four-day experimental period, during which the airflow was maintained within turblent conditions ranging from 0.017 to 0.032 kg/s, as shown in Figure 2.

The pattern observed in all the test days was that the solar intensity and outlet temperature went up early in the morning, reached maximum points around 1:00 PM after which it kept decreasing towards the evening with the lowest values recorded at around 5:00 PM. As depicted in Figure 2, for the paraffin-based solar collectors, the maximum recorded inlet temperature and solar intensity were 23.2 °C and 993 W/m², respectively. The corresponding maximum outlet temperature was 62.9 °C, achieved at the lowest tested airflow rate of 0.017 kilogram per second. Throughout the testing period, environmental conditions remained consistent, with low wind speeds and clear skies, ensuring minimal fluctuations in solar input and reliable performance measurements. From Figure 2 observed phenomenon where the paraffin tube temperature is higher than the outlet air temperature before 12:00 PM, and then becomes lower afterward, can be attributed to the thermal storage and release behavior of the phase change material (PCM). In the morning hours' air flow rate 0.017 kg/s, solar radiation gradually increases, but the airflow rate and ambient temperatures are still relatively low.

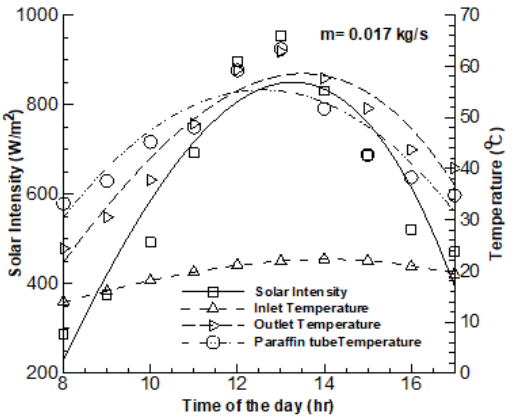

(a)

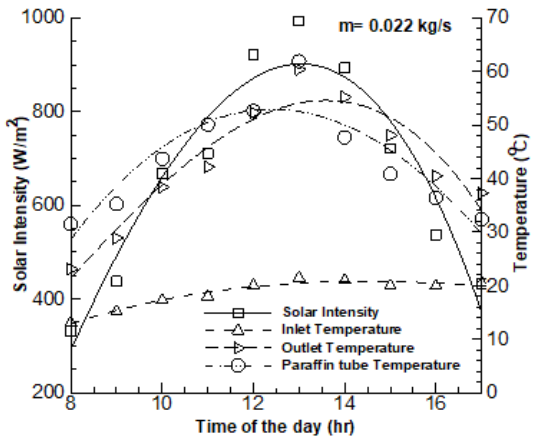

(b)

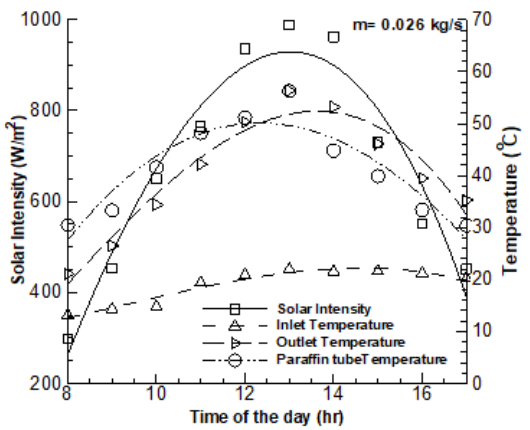

(c)

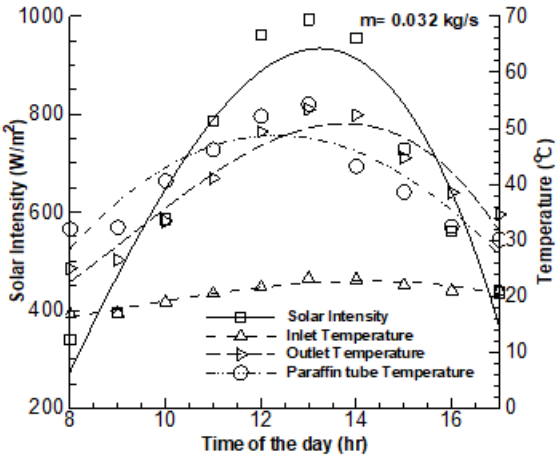

(d)

Figure 2. Variation of solar intensity, inlet, outlet temperatures and paraffin tube temperature to the hours of the day, (a) m= 0.017 kg/s, (b) m= 0.022 kg/s, (c) m= 0,026 kg/s, (d) m= 0.032 kg/s

During this period, the paraffin wax absorbs the incoming thermal energy efficiently and begins to heat up more rapidly than the flowing air, especially since the air has not yet reached peak temperature levels. This results in the paraffin tube temperature exceeding the outlet air temperature before noon. After 12:00 PM, as solar intensity reaches its peak and the air passing through the collector becomes significantly hotter, the outlet temperature increases more rapidly than the temperature of the paraffin. At this stage, the paraffin, having already stored a considerable amount of latent heat, starts to release heat at a slower rate due to its thermal inertia and phase transition characteristics. This thermal effect is similar to the results of work done in the References [3] and [36], who noticed that around the period between 9:00 AM and 10:00 AM, the composite material melts (38.88 ºC) and this process of heating the material commences the latent heat storage. At this stage, the paraffin starts taking in thermal energy but with almost the same temperature. Once 10:00 AM is passed, the temperature of the tubes keeps on increasing and to its maximum between 12:00 PM and 1:00 PM. The temperature in the air moving through the collector becomes much warmer over this period, so the temperature of outlet exceeds the temperature of the paraffin tubes and this represents dynamic thermal exchange and sluggish discharge behavior of the phase change material.

4.2 Dependence of Thermal Parametric Vs. Time of Day

The solar intensity, inlet air temperature, temperature of paraffin tube and outlet air temperature are measured by hourly changes to gauge their dynamic behavior throughout the day during the period of the test. Figure 2 reveals that the intensity of the sun rose steadily starting at the sunrise to reach its peak at around 1:00 PM with maximum reaching about 993 W/m^2 and then it started to go down gradually until the sunset at about 5:00 PM. This was also a pattern of the outlet air and inlet temperature. Initial temperature was taken as the value of the ambient at the early morning and increased slowly with the rise in solar radiation. There was more increase that is acute in the outlet temperature which peaked at 62.9 °C around the solar noon, especially at lower airflow rates (0.017 kg/s) which gave more time to the accumulation of heat. These are also consistent with the findings in the study of Brahma B. et al. (2023), who provided a theoretical analysis of a solar air heater equipment with a paraffin wax. As shown, their study found the highest air- mass flow rate was 0.018 kilogram per second, which gave the highest outlet temperature of 60.40 ºC, and the next highest air- mass flow rate was 0.048 kilogram per second, which produced a small marginally lower outlet temperature of 59.35 ºC. This tendency contributes to the tendencies that are often seen, namely, that the reduced airflow rates shall lead to increased temperature differentials (ΔT) though at the cost of reduced energy gain. The wax made of paraffin in the storage tubes had a delaying thermal reaction due to the thermal inertia. It slowly rose in temperature in the morning and remained absorbing heat in an uninterrupted stream of maximum sunshine. In certain instances, the wax temperature was slightly lower than the curve of outlet air temperature, indicating the stage of continuous operation of changing the phase and the heat storage. This phenomenon brings out the use of paraffin tubes in order to stabilize thermal products during changing environmental conditions of the sun [5].

4.3 Temperature Differences (ΔT) Between Outlet and Inlet Air

Figure 3 depicts that the temperature difference (ΔT = Tout - Tin) is a significant parameter of the thermal efficiency of solar air heaters. In the experiment campaign, the ΔT was measured every hour, at 0.017 to 0.032 kg/s at airflow. The findings showed a clear trend of ΔT toward the morning as the

sun was rising with the highest peak at 1:00-2:00 p.m. because the sun intensity and thermal absorption of energy during this time were the highest. The difference in temperature was also observed to be higher when the airflow rates were low mainly because the residence time of the air in contact with the heated absorber surface would be long to enable better heat transfer. Conversely, in case of increased mass flow rate, although increased amount of air was handled, due to decreased exposure time, there was reduced heat gain and thus, ΔT value decreased. The maximum change in temperature was 41 oC with the paraffin-based collector at the flow rate of 0.017 kg /s, which implies high absorption of heat at low flow rate. These are in line with the results provided by Shalaby et al. (2014), who observed that reducing the airflow rate of flat-plate solar air heaters

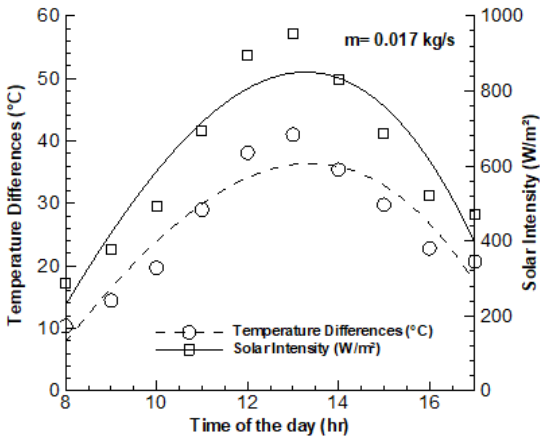

(a)

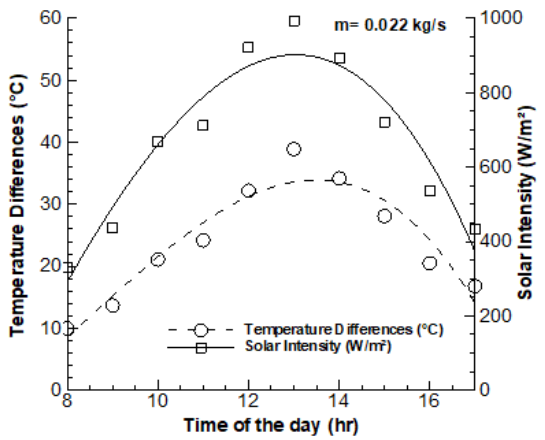

(b)

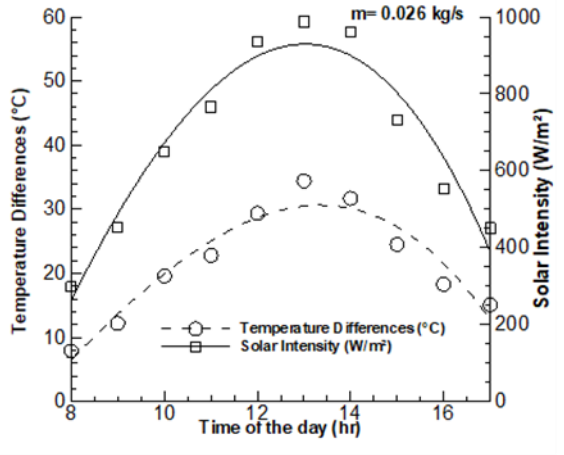

(c)

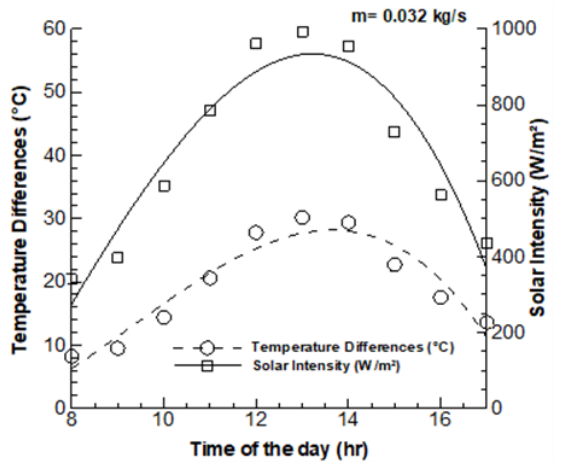

(d)

Figure 3. Dependence of temperature difference (ΔT) on time of day at various airflow rates, (a) m= 0.017 kg/s, (b) m= 0.022 kg/s, (c) m= 0,026 kg/s, (d) m= 0.032 kg/s

contributes widely to improving the temperature of the outlet air after a long heat exchange period. This kind of evidence supports the fact that airflow rate is important in optimization to guarantee balance between thermal efficiency and energy delivery based on the application [15].

4.4. Thermal Efficiency (η)

Figure 4 shows how the thermal efficiency of the two solar collector's changes within a time period of nine hours of an experiment, in different days, and at other airflow rates. Some of the factors affecting the efficiency are environmental and operational such as

ambient temperatures, intensity of solar radiation and heat losses, the speed of wind and the humidity to the environment. Thompson and Reisner (2016) state that thermal efficiency mainly depends on the quantity of useful energy obtained, thus the use of paraffin-filled tubes had great impact on performance improvement. This is believed to be due to the fact that the convective heat transfer rate through the paraffin tubes and between that of the perforated absorber plate and the moving air was enhanced. Increased airflow rates also enhanced the level of heat transfers and energy gain thereby enhancing high level of efficiency. The efficiency curves were the highest at the middle of the day and then the efficiency was high until the end of the day experiments.

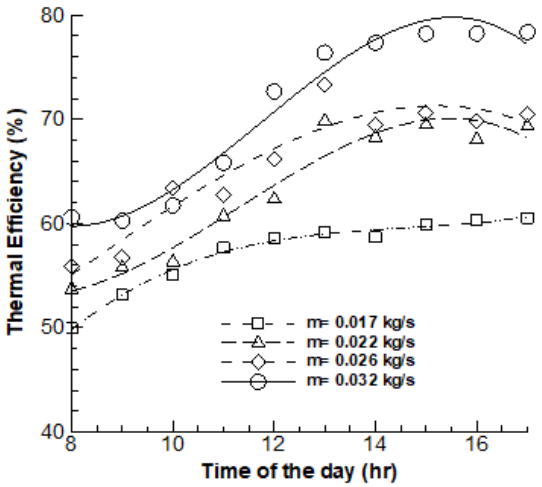

Figure 4. Thermal efficiency variation of the two solar collectors within the entire duration of the experiment at different airflow rates between 0.017 and 0.032 kg/s

It is possible to say that the fact that thermal efficiency curves were the highest at midday, and they were high to the last day of the experiment when it used paraffin tubes could be explained by the thermal storage properties of the phase change materials, in this case, paraffin wax. Throughout the early morning period the solar radiation is slowly rising and the paraffin starts acquiring heat. With increasing ambient temperature and collector temperature, the paraffin will melt and it will change its state and hold the energy, which is latent heat. Later on in the afternoon and early evening, when the sun is not so intense, the stored up energy is given out. This maintains the temperature of the outlets after solar noon as well as the thermal efficiency that continues to operate. This is unlike flat-plate collectors that do not have storage capacity which optimize best during midday and quickly become ineffective as the sun goes down. This led to slower increase in this decrease due to the slow accumulation of paraffin in this study, resulting in a flatter and longer efficiency curve. These results coincide with the study performed by Sohif Mat et al. (2013) which revealed that the instalment of paraffin wax in solar air heaters enhanced the stability and the late-afternoon thermal efficiency of that heaters [32]. Similarly, Shatikian et al. (2005) in a related study discovered that PCM-enhanced collectors worked better to regulate temperature and retain energy particularly when subjected to variations in the solar radiation [33]. In those where a continuous thermal output is needed during the day, it is clear that the use of paraffin tubes is superior to that of non-PCM systems since there can be a long period of high efficiency hours as observed in the study.

5. The Collectors' Useful Energy

Under Equation (7), the game time solar collectors are useful energy gain based on the temperature difference between the outlet and inlet air temperature of the respective airflow rate. The strength of the incoming solar radiation has a great effect on this temperature differences. Figure 5 below shows a relationship for the useful energy picked off inside collectors and a sun radiation over the course of the experiment at different burial of airflow. The temperature rises of the air across the collector, along with the mass flow rate, are the two primary factors governing the amount of useful heat gained. Higher solar intensity produces a larger temperature difference, thereby improving the overall thermal output of the system. The useful energy gain curve shown in Figure 5, that the useful energy gain curve follows a similar curve to that of the solar radiation with the highest value was found around 1:00 PM when the sun irradiance is the greatest. The highest useful energy of the glazed collector was 942.7 W, which is a maximum heat flux of the sun of 988 W/m², when the airflow rate reached maximum of 0.032 kilogram per second. For both collectors, the lower rates of airflow were mean that there an increase in the difference in temperature as well as not increase in the useful energy per kg of air. Nevertheless, an increased rate of airflow resulted in a larger total heat transfer as the amount of air processed increased. This suggests that the greater the

amount of solar energy input and the best airflow gives an efficient heat extraction form a system.

The observation that useful energy produced at the end of the day is more than that produced in the morning of the current study is in line with the previous research studies on solar air heaters that incorporate the use of paraffin wax as a phase change material (PCM). Such phenomenon is explained by the fact that paraffin wax has a thermal storage capacity that absorbs excess heat when the sun is most active (usually it is between 11:00 AM and 2:00 PM) and so releases the heat slowly after the solar input entry begins to decrease. During the mornings of the day, the paraffin is at first in solid state and it takes time to get a satisfactory amount of thermal energy to melt. Due to this, the energy accumulated in the morning is not large. Nevertheless, as soon as the paraffin starts to melt in the middle of the day, it retains large quantities of latent heat. This accumulated energy is released gradually during the afternoon especially during the 2:00 PM-5:00 PM time, keeping the outlet temperatures higher and extending the heat transfer to the air despite the reduction of the solar radiation. This causes more energy gain in the late afternoon than in the morning which is evident in the present day experimental results. Such thermal characteristics are in line with the results of Abdulmunem R. et al. [6] and Aboul-Enein et al. [34] who established that solar air heaters with paraffin wax were able to provide protracted heat delivery during the afternoon, owing to slow rates at which stored thermal power is released [34]. Similarly, as noted by Embiale and Gunjo [1], PCM-

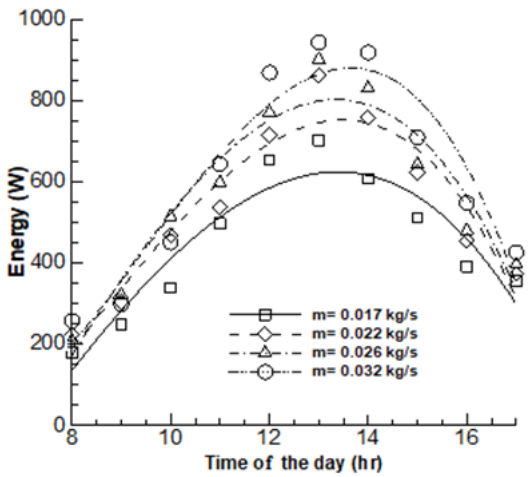

Figure 5. Daily fluctuation of useful thermal power and sun intensity at airflow rates of 0.017 to 0.032 kg/s

based systems provide a buffering capability, can minimize temperature fluctuations, and provide a more stable and lasting thermal output, which helps a lot in the end of the day when the sun is reducing its intensity [1]. Therefore, the commonality in the energy gain pattern realized in this work supports the usefulness of paraffin wax in improving thermal energy consumption during daytime especially retaining high performance levels to the end of the day when the traditional systems have their performance decreasing.

5.1 Influence of Air Flow Rate on Useful Energy Gain, Thermal Efficiency and Heat Removal Factor (ΔT/I)

Figure 6 shows a relationship that exists between airflow rate and the key performance indicators of the solar air heaters that are the heat removal factor (ΔT/I), beneficial energy gain, and thermal efficiency. Heat removal factor which is a ratios of the difference in temperature (ΔT) to the solar light, I, is used to indicate the capacity of system to transfer thermal power on the collector surface. With the airflow rate changing by 0.017 to 0.032 kg/s, a slow decrease in the ΔT/I was noticed. This is normal because the more the degree of mass flow the lower the residence time of air in the collector causing less temperature increment despite carrying more energy since the air has more volume. Conversely, the useful gains of energy and thermal efficiency were both on a rise with the airflow rate. This comes because of the improved convective heat transfer at the absorber surface (and the paraffin tubes in the case of PCM-enhanced collector) and the moving air. When the flow rate is increased, the air in higher flow rate would not gain temperature much as the total heat that is being forced to the air mass increases thus the system operates better. These results indicate the trade-off between flow rate and temperature rise low flow rates produce high, and in terms of total energy gain, high temperature rises are found to be lower, whereas high flow rates produce greater amounts of energy extraction, and thermal efficiency. Thus they are more acceptable in real-world heating use cases

where total energy production is a more significant concern [25], [35].

5.2 Heat Loss Characteristics of a Solar Heater Collectors:

As shown in Figure 7, thermal energy losses in a solar heater collectors are mainly attributed to radiative, convective, and conductive mechanisms. These losses occur from the perforated absorber area and paraffin tubes surface to the surrounding environment.

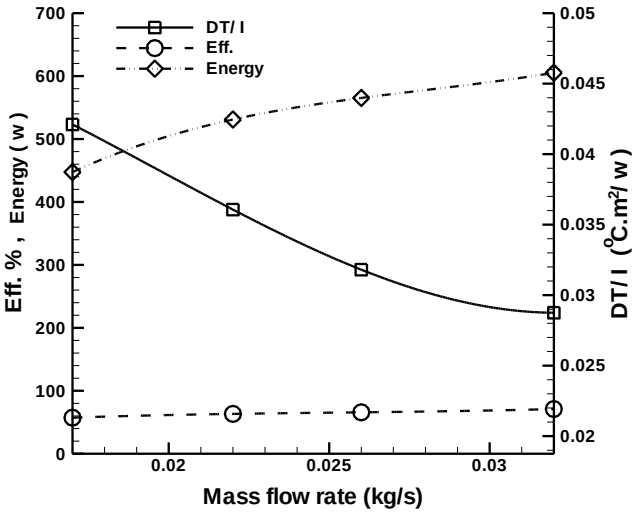

Figure 6. Variation of the heat removal factor (ΔT/I), useful thermal energy gain, and thermal efficiency as a function of air flow rate

The most significant heat losses through the glazed cover by radiation and conviction, while heat losses from the back and side walls was neglected. Such heat losses negatively impact the system's overall thermal efficiency by reducing the amount of useful energy retained and transferred to the working fluid [25].

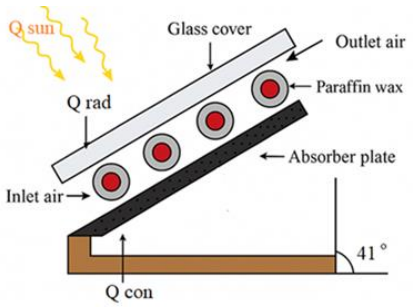

Figure 7. Heat losses due to Convection and Radiative

The overall heat loss from a solar air collector (as shown in Figure 7) is composed of three main components: convective Q_{conv}, radiative Q_{rad}, and conductive heat losses Q_{cond}. The total thermal loss can be expressed as [25]:

$$Q_{loss} = Q_{conv} + Q_{rad} + Q_{cond} \quad (7)$$

5.2.1 Heat Loss Due to Convection

Convective heat losses occur due to convection between the air passing across the collector and the external surface of the collectors, typically a glazed cover. To estimate these losses, the convective heat transfer coefficient for a glazed surface with the ambient environment is calculated by the following empirical formula [25]:

$$Q_{conv} = h_c \times A \times (T_{cover} - T_a)$$
$$where: h_c = 3.8 * \dot{v} + 5.7 \quad (8)$$

For an average wind speed of 5 m/s, then calculated heat transfer coefficient is 22.01 W/m²·K. Based on the different ambient temperature and the varying glass temperature, the value was used to estimate the convective heat loss of the glass cover to the ambient environment to be 164 W.

5.2.2 Radiative Heat Loss

Radiative losses are caused by infrared radiations that are being emitted to the cooler sky by the hot collector surface. One is the net radiative heat transfer and is obtained by the Stefan-Boltzmann law: Radiative Heat Losses: These losses are due to the emission of infrared radiation into the cooler sky by the warm collector surface and the calculated value of this is about 187 w [25].

$$Q_{rad} = \varepsilon \times \sigma \times A \times (T_{cover}^4 - T_a^4) \quad (9)$$

σ: = 5.67×10−8 W/m²·K⁴ (Stefan–Boltzmann constant) and ϵ: Emissivity of the surface (typical value for glass: 0.9)

5.2.3 Conductive Heat Loss

Conductive losses Here, it is obtained in the sidewalls and back insulation of the collector body. The collector that was made in this study had a wooden construction and insulating the walls and the

bottom, which have low thermal conductivity. The conductive heat losses are therefore said to be negligible. It is a deliberate attempt to reduce this pathway by the design in order to preserve a greater amount of thermal energy in the system and increase the overall collector efficiency [25].

$$Q_{back} = U_{back} \times A \times (T_{collector} - T_a) \qquad (10)$$

Since these sections were made of wood that is in itself a low thermal conductor, these sections were constructed in this manner. Wood would be a good resistant to heat loss to the environment. Thus, losses due to these areas are regarded to be irrelevant with the losses due to the glazed surface on the front.

The amount of heat lost according to Equation (7) is: Q_{loss} = 164 W + 187 W + 0 W =351 W. A single collector has an average useful thermal energy of about 447.5 W and the two collectors give a total of 895W with an airflow rate of 0.017 kg/s. The corresponding thermal efficiency loss due to heat transfer is then estimated as: $\eta_{loss} = Q_{loss} / (Q_{useful} + Q_{loss}) = 296 / (895 + 296) \approx 24$ %. Table 3 shows the detailed breakdown of the heat losses and performance losses of the efficiency at each of the airflow rates that were used in the experimental study.

Table 3. Tabular presentations of heat loss components and estimations of thermo-losses in heat along with losses in thermal efficiencies at varying air flow rates

ṁ (kg/s)	Q_{useful}	Q_{conv} (w)	Q_{rad} (w)	Q_{loss} (w)	η_{loss} %
0.017	895	109	187	296	24
0.022	1062	82	170	252	19
0.026	1130	76	157	233	17
0.032	1210	68	137	205	14.5

As the air mass flow rate (ṁ) is doubled (from 0.017 kg/s to 0.032 kg/s) the system is observed to respond with an observable increase in useful thermal energy production, growth in total thermal losses getting lower with a decrease in both convective and radiative heat losses down to 296 W and 205 W respectively. Such lessening number of losses is expressed in the lowering of loss percentage, which decreases as much as 24 percent at lowest rate of flow, down to 14.5 percent at highest.

5.3 Effect of Air Flow Rate on Thermal Energy Gain, Heat Loss, and Outlet Temperature

Figure 8. shows that the experimental data points out that the total thermal energy acquired remains constant with increasing the air flow rate of 0.017 to 0.032 kilogram per second taking a form of a steady increase to more than 39 MJ at the highest rate of air flow. This however, is at a minimal cost in outlet air temperature as the air residence time limitation in the collector is minimized. Nonetheless, the entire heating capacity is enhanced due to the increased amount of processed air. Loss of heat on the other hand reduces, slightly with increasing flow rate leading to efficient system operation. These findings point to a trade-off between the temperature of an outlet and the amount of heat delivered. The reduced rates of airflow produce high temperatures at the outlet, hence suitable in focused or small area heating, but increased mass of gas flow rates is beneficial in large area heating because of the greater overall energy absorption, and also much minimized heat losses.

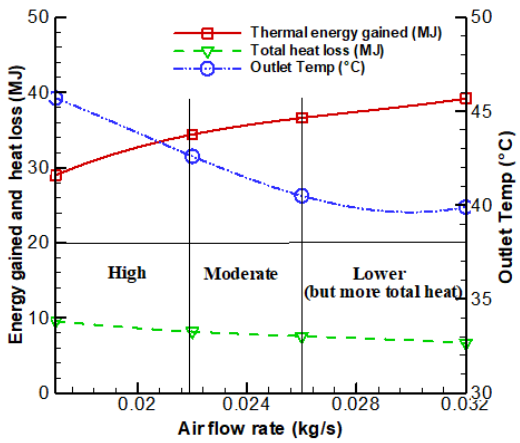

(a)

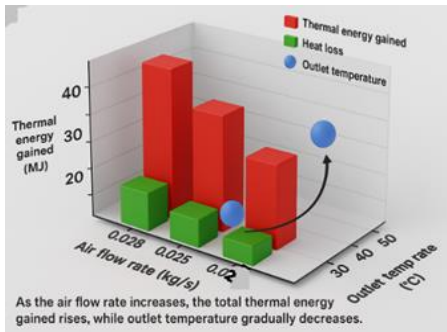

(b)

Figure 8. Effect of Airflow rate on variation of Energy Gain, Heat Loss and the Outlet Temperature in a Solar Air Heater, (a) 2D and (b) 3D

5.4 Effect on Pressure drop and Mechanical Power demands, Full Development: Flow Regime

The change in pressure loss across the collector when air is passed through it can be described as pressure drop caused by friction, hindrances (perforated plates, paraffin tubes) and size changes. When high-pressure drop it means that, it has greater resistance and it therefore needs more fan power in order to sustain the airflow. It has an indirect impact on thermal performance heat transfer is limited by confined airflow. The Darcy–Weisbach equation [36] was used to calculate the pressure drop (ΔP) of the air flowing through the collectors [30]:

$$\Delta P = f \times (\frac{L}{Dh}) \times (\rho \times \frac{v^2}{2}) \quad (11)$$

Where: L=1.09 m is the duct length, Dh= 0.1495 m is hydraulic dimeter and volumetric flow rate V = 1.014 ṁ/ρ, (ρ is air density 1.127kg/m^3). In the case of laminar flow (Re < 2300), f was determined with [36]:

$$f = 64/Re \quad (12)$$

To determine the empirical correlation when turbulent flow (Re > 2300) was taken, the empirical correlation was used [36]:

$$f = 0.085 \times Re^{-0.25} \quad (13)$$

The power (w) that is required by a fan or blower to circulate air through the system overcoming the pressure difference is known as mechanical power [37]. with the fan efficiency assumed to be $\eta_{fan} = 0.65$.

$$W = (\Delta P \times V)/\eta_{fan} \quad (14)$$

Table 4. Effect of Flow Regime on Friction Factor, Pressure Drop, and Mechanical Power Consumption

Flow	ṁ	Re	f* 10^{-2}	**Δ**P*10^{-3}	W_{mech}*10^{-3}
laminar flow	0.017	1506	425	48	0.111
laminar flow	0.022	1949	328	62	0.186
Turbulent flow	0.026	2304	122	32	0.114
Turbulent flow	0.032	2835	116	46	0.209

Based on the practical system design view (Table 4), the obtained results reveal the influence of air mass flow rate variation on the pressure drop and the mechanical power demand of a solar air heater. At lower flow rates (0.017-0.022) kilogram per second, the system is in the laminar regime where increased factors of friction (0.0425 and 0.0328) lead to increased pressure drops. The resistance needed (0.00011-0.000186 W) is very small but the resistance that is increased could reduce the uniformity of airflow and the performance of heat transfer. With further increased of the flow rate over 0.026 and 0.032 kilogram per second, a flow enters a turbulent regime, and the friction factor decreases significantly (to about 0.012), which is accompanied by lower pressure losses at higher velocities. Such conduct has an advantage in the agile design since it can gain an increased thermal performance and airflow under the condition of a relatively small rise in fan energy. These results indicate that running in the turbulent flow regime or close to it can lead to a more efficient system operation through the attainment of high convective heat transfer and airflow distribution at minimal increases in energy demand thereby being a good environment to optimize the performance of solar air heaters [7].

5.5 An Active Heating System Integrated with a Solar Air Heater:

In order to calculate the area and height of a workshop that can be effectively warmed with the help of two collectors under turbulent flow conditions, with the air flow rate ranging between 0.026 and 0.032 kilogram per second total useful thermal energy output was contrasted with the energy necessary to keep the appropriate temperature and ventilation levels indoors. It is commonly approximated that a space heating that relies on heat production needs the calculation of Equation (15) [25]:

$$Q = V.\rho.C_p.\Delta T \quad (15)$$

The dimensions of the workshop in this case are 20×15×4 m which make the total volume of 1200 m3. The overall energy of heat collected by the system in 0.032 kg/s of airflow is 39 MJ and when losses of 6.64 MJ of heat are taken into consideration, the final amount of useful energy that can be obtained is some 32.36 MJ. This energy can get the air a temperature comparable to 10 oC in a space of about 2,677 m3. Therefore, based on the reported information and net

energy savings, we can conclude under the circumstance that the two solar collectors will be able to heat two workshops with a volume of 1,200 m3 each.

5.6 Energy Savings, Environmental Impact, and Cost Feasibility over the System Lifetime

The paper evaluates the thermal performance, energy-saving and environmental benefit of two solar-driven air heating systems integrated in a functional ventilation and heating system over a long period. In the evaluation, it is based on experimental data collected under real climatic conditions including measurements of thermal energy output, heat losses as well as changes in the airflow rates [38]. The life cycle assessment (LCA) looks at how well the system works in the winter, which is from October to March, when people need the most heat in the area. Every day during the day, the system was run, and the temperature of the air coming in and going out, the intensity of the solar radiation, and the flow rate of the air mass were measured every hour. Assuming a daily operation time of 9 hours for 180 days per year, the total annual operational time amounts to 1,620 hours/year. With an average measured useful thermal output of 1,210 W, the total annual energy contribution is calculated as [25]: 1210 W× 1620 hours= 1,960,200 Wh = 1960 kWh/year = 7.06 GJ/year.

To estimate the system's impact on greenhouse gas emissions, Iraq's thermal-energy emission factor (kg CO_2 /MJ) for diesel 0.074 kg CO_2 /MJ and 0.056 kg CO_2 /MJ for natural gas, as reported by the IPCC). The annual CO_2 reduction achieved through this system is: 1960 kWh/year × 3.6 MJ/kWh=7056 MJ/year. CO_2 (diesel) = 7056×0.074=522.1 kg CO_2 /year. CO_2 (natural gas) = 7056×0.056=395.1 kg CO_2 /year. This decrease is specifically high in the Iraqi scenario when the fossil fuels are the major source of electricity production and thus this is where solar thermal systems are of great importance to the environment. The feasibility of the economy is determined with the help of the Formula-Payback period (years) = System Cost/Annual Savings. An estimate of annual savings was made assuming the price of electricity is $0.10/kWh:1960 kWh/year × $0.10/kWh = $196/year. The anticipated payback period is 2.5 to 3 years with an assumed cost of the system of between 500 and 600. This goes to show that, the proposed system is not only friendly to the environment, but also cost effective where long-term heating is concerned.

6. Validation and Comparison with Previous Studies

The findings of this study were validated by comparing them with previously published work on PCM-enhanced solar air heaters. As presented in Table 5, the proposed system achieved a markedly higher temperature rise of 58 °C and the highest thermal efficiency of 78%, outperforming earlier designs that reported temperature increases of 15–22 °C and efficiencies ranging from 50% to 70%.

The improved performance of the present system compared with previous studies operating at the same mass flow rate of 0.032 kg/s is primarily attributed to the advanced design of the perforated absorber plate together with the transparent glazing. This configuration enhances heat transfer between the absorber surface and the flowing air. The perforations promote better airflow mixing and increase residence time, resulting in a higher temperature rise without a significant increase in pressure loss. Additionally, the glazing layer minimizes heat losses to the surroundings, allowing a greater portion of the absorbed solar energy to be delivered as useful thermal output. When combined with the higher available solar radiation, these design improvements lead to superior thermal efficiency and overall system performance compared with the previously reported PCM-based solar air heaters.

The present study proposes a novel perforated absorber configuration integrated with a PCM-supported dual-pass airflow system, resulting in a markedly higher temperature rise, enhanced thermal efficiency, longer heating duration, and notable environmental advantages compared with previously reported PCM-based solar air heater designs.

Table 5. Comparison with previously published work

Researcher	Collector Type	A m^2	I w/m_2	**Δ**T oC	η%
B.N. Abdullah [39]	V-Corrugated absorber, Paraffin-wax	2	870	16	65
Salah M. Salih [17]	Rectangular capsules, Paraffin-wax	0.41	625	15	50

Singh A. K. [7]	Serrated geometric, Paraffin-wax	1.62	710	18	63
Embiale D.T [1]	Double-pass, Paraffin-wax	36.12	950	22	70
Present work	perforated plate, glazed cover	1.24	987	58	78

7. Conclusion

This research project experimentally examined thermal performance and storage capacity of energy as well as the practical heating of the air using the dual solar air heater system combined with the use of paraffin wax tubes. These findings showed that accelerating the airflow rate between 0.017 kg/s to 0.32 kg/s had a great effect of increasing total useful thermal energy production to a maximum 39.2 MJ/day together with decreasing the percentages of heat losses down from 24% to 14.5 percent. Despite an insignificant drop in air outlet temperature further caused by higher flow rates, the thermal efficiency was improved in general as there was an increase in mass flow and enhanced convective heat transfer.

After taking into consideration losses, the system had a net daily energy gain of 32.36 0 MJ and this energy gain is enough to increase the space of about 2677 m3 in indoor temperature by 10 oC. This demonstrates that the dual-collector system has the potential to warm up two conventional workshop areas (1200 m3 each) during cool winter periods.

Moreover, the estimated annual energy saving at the power charge of $0.10 per kWh is 196, and with a payback period value of between 2.55 and 3.06 years, the economic payback period of the system varies according to the initial cost of the system. The CO2 emission savings were estimated at 522.1 kg CO2/year and 395.1 kg CO2/year of diesel and natural gas respectively, according to the national grid emissions factor in Iraq, further supporting the role of using such systems in the fossil fueled geographical areas in promoting environmental well-being.

Conclusively, paraffin wax that is incorporated as a phase change material into solar air heaters can considerably decrease thermal loss, improve energy storage, enable efficient space heating, and has a short payback period hence it is a promising as a solution that will be useful in the heating of buildings with a similar climatic condition.

Future developments in this research will involve investigating thermal-storage materials other than paraffin wax, particularly nanomaterials that offer extended heat-retention capabilities. Furthermore, a comprehensive numerical study using CFD will be conducted to analyze and validate the system's thermal behavior in greater detail.

Nomenclature

a	Duct area (m^2)
A	Surface area of collector (m^2)
Dh	Hydraulic diameter of the collector (m).
F'	Plate removal factor (-)
f	Friction factor (-)
Fo	Ratio of the actual useful heat gain to the maximum possible heat gain (-)
hc	Convective heat transfer coefficient between cover and ambient ($W/m^2 \cdot °C$)
L	Length of air flow passage(collector length) (m).
I	Solar intensity (W/m^2)
A_P	Surface area of absorber plate (m^2)
$\dot{m}$	Air flow rate (kg/s)
Q	Required heat energy (W)
Q_u	Useful heat gain (W)
Q_{loss}	Total heat loss from the collector (W)
	Conductive heat loss through collector materials (W)
Q_{conv}	Convective heat loss from the top cover to ambient (W)
Q_{rad}	Radiative heat loss between the cover and sky (W)
Q_{cond}	Conductive heat loss through collector materials (W)
Q_{back}	Heat energy loss of a back collector ($W/m^2 \cdot °C$)
U_{back}	Coefficient of heat loss of a back collector ($W/m^2.°C$)
Re	Reynolds number (-)
T_i	Inlet air temperature (°C)
T_a	Ambient temperature (°C)
T_{cov}	Glass cove temperature (°C)
T_o	Outlet air temperature (°C)
T_{coll}	Collector temperature (°C)
v	Volumetric flow rate of air (m^3/s)

v	Air velocity (m/s)
v'	Wind speed over the collector (m/s)
W	Mechanical power, fan power requirement (W)
$\tau\alpha$	Effective transmittance absorbance (-)
η	Efficiency (-)
η_{fan}	Fan efficiency (-)
η_{th}	Thermal efficiency (-)
ρ	Density of air (kg/m^3)
σ	Stefan–Boltzmann constant (W/m^2.^{o}C^4)
ε	Emissivity of the surface (-)
$\omega\eta$	Absolute uncertainty in efficiency (-)
$\omega\dot{m}$	Absolute uncertainty in mass flow rate (-)
$\omega\Delta T$	Absolute uncertainty in temperature rise (-)
ωI	Absolute uncertainty in solar irradiance measurement (-)
ωv	Absolute uncertainties in velocity (-)
ωa	Absolute uncertainties in duct area (-)
$\omega\rho$	Absolute uncertainties in density (-)
ΔP	Pressure drop of air through the collector (N/m^2).
ΔT	Temperature differences (^{o}C)
Cp	Specific heat of air (KJ/kg. °C)
$IPCC$	Intergovernmental Panel on Climate Change

References

[1] Embiale D.T. and Gunjo D.G. (2023). Investigation on solar drying system with double pass solar air heater coupled with paraffin wax based latent heat storage: Experimental and numerical study. Results in Engineering, 20, 101561. https://doi.org/10.1016/j.rineng.2023.101561

[2] Njoku, M. C., Nwosu, P. C., Azodoh, K. A., Gaven, D.V., & Ahaotu, R.O. (2023). Design analysis and material selection of flat-plate solar thermal collectors. In Proceedings of the School of Engineering and Technology Conference and Exhibition(SETCONF). https://www.researchgate.net/publication/370954236

[3] Ibrahim L.I, Ahmed A.Q., Abdulrahman Th. M. and Al-Syyab A.K. (2023). Numerical Study to Investigate the Performance of U-shaped Flat Plate Solar Collector Using Phase Change Materials (PCMs). Journal of Techniques, 5(2), 74-80. https://doi.org/10.51173/jt.v5i2.1302

[4] Mehul, A. M. S., & Ramana, P. V. (2025). A comprehensive review on solar drying using paraffin wax as PCM, J. Renewable Sustainable Energy, 17, 012701. https://doi.org/10.1063/5.0239679.

[5] Jasim, Q. A., Jasim, A. M., Khudhair, A. H., & Chaichan, T. I. (2020). Improve the performance of a solar air heater by adding aluminum chip, paraffin wax, and nano-SiC. Case Studies in Thermal Engineering, 19, 100622. https://doi.org/10.1016/j.csite.2020.100622.

[6] Abdulmunem R.A., Mohammed H. J., Pakharuddin M. S., Hasimah A. R. and Hashim A. H. (2019). Analysis of Energy and Exergy for the Flat Plate Solar Air Collector with Longitudinal Fins Embedded in Paraffin Wax Located in Baghdad Center. International Journal of Heat and Technology, 37(4), 1180-1186. https://doi.org/10.18280/ijht.370428

[7] Singh A. K., Saxena A. and Agarwal N. (2023). Performance analysis of a serrated absorber plate solar air heater with paraffin wax storage. Environmental Science and Pollution Research, 31, 62408–62426. https://doi.org/10.1007/s11356-023-27961-8.

[8] Mahto P.K., Pradhan P.M. and Das P.P. (2023). Experimental Investigation of Solar Air Heater Using Pin Fin Absorber Plate with Pin Immersed in Paraffin Wax. International Review of Mechanical Engineering, 17(9), 425-435. https://doi.org/10.1016/j.tsep.2025.103380.

[9] Soliman A.S., Cheng P., Ahmed A.S., Abdelrehim S.O. and Sultan M.A. (2025). A new design of a bifacial solar air heater with PCM. Thermal Science and Engineering Progress, 59, 103380. https://doi.org/10.1016/j.tsep.2025.103380.

[10] Salah M.S., Jalal M. J. and Saleh E. N. (2019). Experimental and numerical analysis of double-pass solar air heater utilizing multiple capsules PCM. Renewable Energy, 143, 1053-1066, https://doi.org/10.1016/j.renene.2019.05.050.

[11] Fath H.E. (1995). Thermal performance of a simple design solar air heater with built-in thermal energy storage system. Energy Conversion and Management,6(8),1033-1039. https://doi.org/10.1016/0196-8904(94)00069-

[12] Charvát P., Klimeš, L., Pech, O. and Hejčík, J. (2019). Solar air collector with the solar absorber plate containing a PCM– Environmental chamber experiments and computer simulations. Renewable Energy, 143, 731–740. https://doi.org/10.1016/j.renene.2019.05.049

[13] Agyenim F., Eames P. and Smyth M. (2010). Heat transfer enhancement in medium temperature thermal energy storage system using a multitude heat transfer array, Renew Energy, 35, (1), 198-207. https://doi.org/10.1016/j.renene.2009.03.010.

[14] Tyagi V., Panwar N.L., Rahim N.A.and Kothari R. (2012). Review on solar air heating system with and without thermal energy storage system. Renew. Sustain. Energy Rev, 16 (4), 2289-2303. https://doi.org/10.1016/j.rser.2011.12.005.
[15] Shalaby S., Bek M.A. and El-Sebaii A.A. (2014). Solar dryers with PCM as energy storage medium: a review Renew, Sustain. Energy Rev., 32, 110-116. https://doi.org/10.1016/j.rser.2014.01.073.
[16] Acır A.and Canlı M., E. (2018). Investigation of fin application effects on melting time in a latent thermal energy storage system with phase change material (PCM), Appl. Therm. Eng.14, 1071-1080. https://doi.org/10.1016/j.applthermaleng.2018.09.013.
[17] Salah M. Salih, Saleh E. N. and Jalal M. J. (2019). Numerical Modeling for Novel Solar Air Heater Utilizing Wax Paraffin-PCM. Basrah Journal for Engineering Sciences, 19, (2), 1-8. https://doi.org/10.33971/bjes.19.2.1.
[18] Alam T., Saini R. P., and Saini J. S. (2014). Experimental investigation of thermohydraulic performance of a rectangular solar air heater duct equipped with v-shaped perforated blocks. Advances in Mechanical Engineering, 948313- 11. https://doi.org/10.1155/2014/948313.
[19] Matsunaga J., Kikuta K., Hirakawa H., Mizuno K., Tajima M., Hayashi M. and Fukushima A., (2021). An Assessment of Heating Load Reduction by a Solar Air Heater in a Residential Passive Ventilation System. Energies 14, 7651. https://doi.org/10.3390/en14227651.
[20] Singh S., Hander S. and Saini J.S. (2012). Investigations on thermohydraulic performance due to flow-attack-angle in V-down rib with gap in a rectangular duct of solar air heater. Applied Energy, 97, 907–912. https://doi.org/10.1016/j.apenergy.2011.11.090.
[21] Sara O. N., Pekdemir T., Yapici S., and Ersahan H. (2000). Thermal performance analysis for solid and perforated blocks attached on a flat surface in duct flow. Energy Conversion and Management, 41(10), 1019–1028. https://doi.org/10.1016/S0196-8904(99)00163-6.
[22] Shin S. and Kwak, J.S. (2008). Effect of hole shape on the heat transfer in a rectangular channel with perforated blockage walls. Journal Mech. Sci. Tech., 22, 1945–1951. https://doi.org/10.1007/s12206-008-0736-7.
[23] Pandey R. and Kumar M. (2021), Efficiencies assessment of an indoor designed solar air heater characterized by V baffle blocks having staggered racetrack-shaped perforation geometry. Sustain. Energy Technol. Assessments. 47, 101362. https://doi.org/10.1016/j.seta.2021.101362
[24] Arunkumar H.S., Shiva Kumar and Vasudeva Karanth K. (2022). Performance enhancement of a solar air heater using rectangular perforated duct inserts. Thermal Science and Engineering Progress, 34, 101404. https://doi.org/10.1016/j.tsep.2022.101404.
[25] Mahmood A.J. (2025). Experimental investigation of thermal efficiency, heat losses, and economic, Results in Engineering, 27, 106004. https://doi.org/10.2139/ssrn.5269685.
[26] Lafta N.S. Mahmood A.J., Jehhef, K.A. and Kareem F.A. (2025). Solar Thermal Performance: Using Perforated, Corrugated, Waved and Punched Absorber Plates. Engineered Science, 34, 1435. https://doi.org/10.30919/es1435.
[27] Mahmood A.J. (2021). Experimental study for improving unglazed solar system. Cogent Engineering, 19615641 (8), 1–17. https://doi.org/10.1080/23311916.2021.1961564.
[28] Kareem F.A., Lafta N.S. and Mahmood A.J. (2023). Numerical investigation flat plate solar collector performance in Baghdad base on exergy analysis. Int. J. Exergy, 42, (1). https://doi.org/10.1504/IJEX.2023.134286.
[29] Mahmood A.J. (2019). Exergy Analysis of Flat Plate Solar Air Heaters Having Obstacles and Filled with Wire Mesh Layers. Iop Conference Series Materials Science and Engineering, 518 (3), 032001. https://doi.org/10.1088/1757-899X/518/3/032001.
[30] Mahmood A.J., Aldabbagh L.B.Y. and Egelioglu F. (2015). Investigation of single and double pass solar air heater with transverse fins and a package wire mesh layer. Energy Conversion and Management, 89, 599–607. https://doi.org/10.1016/j.enconman.2014.10.028.
[31] Brahma B., Shukla A.K. and Baruah D.C. (2023). Design and performance analysis of solar air heater with phase change materials Author links open overlay panel. Journal of Energy Storage, 61, 106809. https://doi.org/10.1016/j.est.2023.106809.
[32] Sohif Mat S., Bduljalil A. Al-Abidi, Sopian K., Sulaiman M.Y. and Abdulrahman Th.M. (2013). Enhance heat transfer for PCM melting in triplex tube with internal–external fins. Energy Conversion and Management, 74, 223-236. https://doi.org/10.1016/j.enconman.2013.05.003
[33] Shatikian V., Ziskind, G. and Letan, R. (2005). Numerical investigation of a PCM-based heat sink with internal fins. International Journal of Heat and Mass Transfer, 48 (10), 2162–2172. https://doi.org/10.1016/j.ijheatmasstransfer.2004.10.042.

[34] Aboul-Enein S., El-Sebaii A., Ramadan M. and El-Gohary H. (2000). Parametric study of a solar air heater with and without thermal storage for solar drying applications. Renewable Energy, 21, 505- 522. https://doi.org/10.1016/S0960-1481(00)00092-6.
[35] Mahmood A.J., Lafta N.S., Kareem F.A. and Majeed J.H. (2025). Exergy Analysis of a double pass glazed solar heater with corrugate perforated Absorber Plate: An Experimental Study. (5th International Conference on Sustainable Engineering Techniques (ICSET24)), IOP Conf. Series: Earth and Environmental Science. 1507, 012007. https://doi.org/10.1088/1755-1315/1507/1/012007.
[36] I.L, Ihnayyish1 Ahmed A.Q., Mohammad A.Th. and Al-Syyab A. k. (2023). Numerical Study to Investigate the Performance of U-shaped Flat Plate Solar Collector Using Phase Change Materials (PCMs), Journal of Technique, 5 (2), 74-80. https://doi.org/10.51173/jt. v5i2.1302.
[37] Duffie J.A. and Beckman W.A. (2013) Solar Engineering of Thermal Processes, 4th ed., Wiley.
[38] Elnaggar M. (2023). Useful energy, economic and reduction of greenhouse gas emissions assessment of solar water heater and solar air heater for heating purposes in Gaza, Palestine. Heliyon, 9, e16803.
https://doi.org/10.1016/j.heliyon. 2023.e16803.
[39] Abdullah B.N., Almerane A.E. and Khaleel O.S. (2023). Energy Conversion of V-Corrugated Absorber Plate Solar Air Heater with Phase Change Material. Technical and Physical Problems of Engineering, 15 (3), 135-142. https://www.researchgate.net/publication/374738516